Ion kinetics in a magnetized plasma source

Boris N. Breizman and Alexey V. Arefiev
Institute for Fusion Studies, The University of Texas, Austin, Texas 78712

(Dated: September 13, 2001)

Abstract

There are regimes of plasma source operation in which the ion motion is controlled by the ambipolar electric field and ion-atom collisions. This paper presents a derivation of the corresponding ion distribution function and plasma density profiles in the source for a given electron temperature and a given gas ionization rate. Conditions are discussed under which the ion flux is predominantly radial or predominantly axial. It is found that the presence of plasma can substantially change the neutral gas pressure due to production of fast charge-exchange neutrals.

52.25.Dg, 52.25.Fi, 52.50.Dg, 52.55.Dy

I. INTRODUCTION

This work is an attempt to address the physics of plasma flow formation in magnetized plasma sources, of which a helicon source is a typical example. Helicon sources are known for their remarkably high efficiency [1, 2], which stimulates numerous applications ranging from plasma materials processing [3–5] to plasma thrusters for space propulsion [6, 7]. The need to develop a credible physics model of the helicon sources has generated an extensive theoretical effort [8–12]. Nevertheless, some pieces of the puzzle still don't quite fit-in and some may still be missing.

The immediate practical motivation for our study is the VASIMR Plasma Thruster project [7], which involves the use of a light-ion helicon source. However, this paper deals more with the basic physics aspects than with a particular device. Therefore, some of the features that we discuss below are not unique to helicon sources.

In what follows, we will consider a schematic layout shown in Fig. 1. We will assume that the plasma is created via rf-discharge inside an axisymmetric dielectric tube placed in a uniform axial magnetic field (B_0). The tube length (L) is much greater than the radius (a). One end of the tube is sealed by an emissive metal plate with an opening for gas injection. The other end is open into a vacuum to allow free plasma flow out of the source.

We will limit our consideration to the case of rarified gas with the particle mean free path larger than the tube radius. A Knudsen-type gas flow will then establish itself in the tube in the absence of plasma. The gas density in this flow is uniform over the tube cross-section and decreases linearly from its maximum value at the end-plate to nearly zero at the open end. We will assume that the gas is monatomic and that the degree of ionization is small in the rf-discharge. The latter will allow us to neglect any plasma effect on *the gas density profile*. We will however be able to describe an increase in *the gas pressure* associated with fast charge-exchange neutrals (see Sec. V).

The problem of plasma flow is essentially a kinetic problem of ion transport. The ion motion in the discharge is controlled by: (1) ambipolar electric field resulting from quasineutrality; (2) equilibrium magnetic field; (3) ion collisions with atoms. As the ion density is

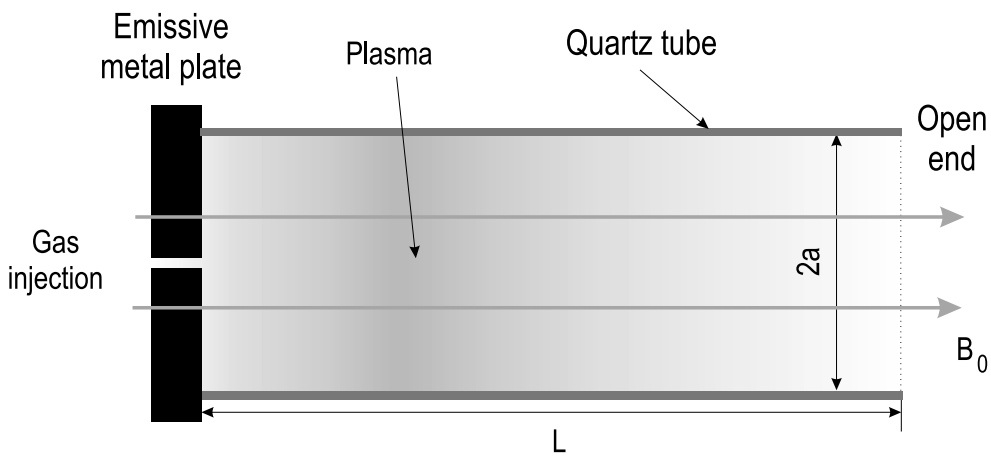

FIG. 1: Schematic layout of magnetized plasma source.

small compared to the gas density, we neglect ion-ion collisions compared to ion-atom collisions. The ion density profile is generally nonuniform in both longitudinal and radial directions since the ions are confined radially by the magnetic field. As a result, the ambipolar electric field, associated with the ion density gradient, has both longitudinal and radial components.

It should be noted that description of ion transport requires information about electrons. We need to know electron temperature to relate the ambipolar electric field to the ion density profile. Another important "electron" parameter in our problem is the gas ionization rate by electron impact. The ionization rate may not be determined by the bulk electron temperature since fast electrons are not necessarily Maxwellian. However, we will not discuss electron kinetics in this work. Instead, we will use a more limited approach: we will treat the bulk electron temperature and the ionization rate as input parameters. The results of this analysis should ultimately be combined with a proper kinetic description of electrons to give a self-consistent model of the discharge. Macroscopically, we will concentrate on the particle balance, while the electron kinetics is more a power balance issue.

The rest of the paper is organized as follows. In Sec. II, we present a qualitative discussion of ion transport to obtain simple estimates for the longitudinal and radial particle fluxes and the corresponding confinement-times. In Sec. III, we derive the gyro-averaged ion distribution function in presence of an ambipolar electric field and ion-atom charge-exchange

and elastic collisions. This solution allows us to quantitatively evaluate ion fluxes. In Sec. IV, we find the density profiles in steady-state plasma flows. Here, we consider the limiting cases of longitudinal and radial losses. We also formulate the conditions under which a steady-state is allowed. Finally, in Sec. V, we discuss limitations of our model and some implications of our results.

II. QUALITATIVE ESTIMATES OF THE ION TRANSPORT

Ion transport in the discharge is controlled by equilibrium magnetic field, ambipolar electric field, and ion-atom collisions. The equilibrium magnetic field is typically strong enough to magnetize the ions, so that the following two conditions are satisfied:

$$\rho_{Li} \ll a, \tag{1a}$$

$$\nu \ll \omega_{ci}, \tag{1b}$$

where ρ_{Li} is the ion gyro-radius, a is the plasma radius, ν is the ion-atom collision frequency, and ω_{ci} is the ion gyro-frequency. The longitudinal and radial ion transports are significantly different under these conditions.

The charge-exchange and elastic collisions are the dominant ion-atom collision processes for ion energies up to few eV [5, 13]. In terms of energy and momentum conservation, charge-exchange collisions are essentially equivalent to head-on elastic collisions. Both the charge-exchange cross-section (σ_{cx}) and the elastic cross-section (σ_{el}) are nearly constant in the energy range of interest and they are of the same order of magnitude [5, 13]. We will assume that the gas temperature is much lower than the characteristic ion energy. In this case, the ions lose a significant part of their kinetic energy in each collision. The ion-atom collision frequency is given by

$$\nu = n_0 v(\sigma_{cx} + \sigma_{el}), \tag{2}$$

where n_0 is the gas density and v is ion velocity. The characteristic velocity in Eq. (2) can be estimated as the ion velocity gain in the ambipolar electric field $\mathbf{E}$ between two collisions.

The velocity gain in the direction of the magnetic field ($v_{\|}$) is roughly

$$v_{\|} \approx \frac{|e|E_{\|}}{m_i \nu}. \tag{3}$$

The transverse velocity gain for magnetized ions ($v_{\perp}$) is of the order of the $\mathbf{E} \times \mathbf{B}$-drift velocity ($u_E$):

$$v_{\perp} \approx u_E \equiv \frac{|e|E_r}{m_i \omega_{ci}}. \tag{4}$$

Assuming that the longitudinal and radial scale-lengths of the plasma density profile are L and a, respectively; we estimate $E_{\|}$ and E_r as

$$E_{\|} \approx \frac{T_e}{|e|L}, \tag{5a}$$

$$E_r \approx \frac{T_e}{|e|a}, \tag{5b}$$

where T_e is the bulk electron temperature. We now combine Eqs. (2)-(5) into

$$\nu = n_0(\sigma_{cx} + \sigma_{el})\sqrt{v_{\|}^2 + v_{\perp}^2} \approx n_0(\sigma_{cx} + \sigma_{el})C_s\sqrt{\frac{C_s^2}{\nu^2 L^2} + \frac{C_s^2}{\omega_{ci}^2 a^2}}, \tag{6}$$

where $C_s \equiv \sqrt{T_e/m_i}$ is the ion sound velocity. This estimate for ν can be approximated by the expression

$$\nu \approx \xi(\xi + 1)\frac{a\omega_{ci}}{L}, \tag{7}$$

with

$$\xi \equiv \frac{C_s}{a\omega_{ci}}\sqrt{n_0 L(\sigma_{cx} + \sigma_{el})}. \tag{8}$$

We will now show that the parameter ξ characterizes the ratio between the radial and longitudinal ion fluxes. The mechanism of radial transport is shown schematically in Fig. 2. An initially slow ion is accelerated by the radial ambipolar electric field until its velocity becomes comparable to the drift velocity u_E. Between collisions, the ion drifts in the azimuthal direction and oscillates radially with the radial orbit excursion of the order of $\rho_{Li} \approx u_E/\omega_{ci}$. Every collision replaces the accelerated ion by a slow ion. This effectively

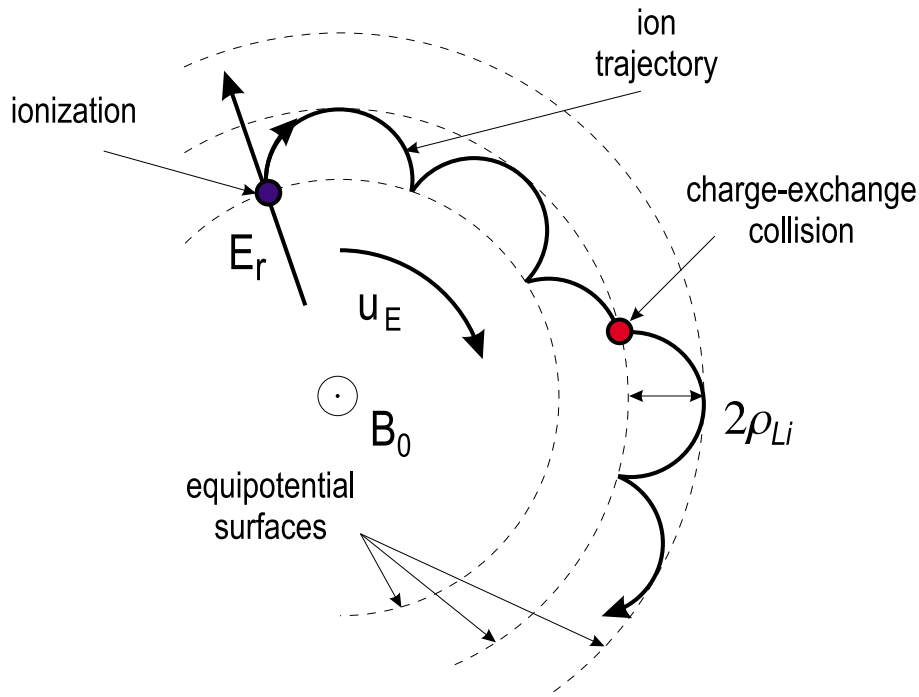

FIG. 2: Ion transport across the magnetic field.

shifts the ion orbit in the direction of the ambipolar electric field by ρ_{Li}. The average radial flow velocity, therefore, can be estimated as

$$u_\perp \approx \nu\rho_{Li} \approx \frac{|e|E_r}{m_i\nu}\frac{\nu^2}{\omega_{ci}^2}. \tag{9}$$

The ensuing expressions for the total radial flux ($\psi_\perp$) and the radial confinement time ($\tau_\perp$) are

$$\psi_\perp \approx nu_\perp aL \approx \xi(\xi+1)na^2C_s\frac{C_s}{a\omega_{ci}}, \tag{10a}$$

$$\tau_\perp \approx a/u_\perp \approx \frac{L}{\xi(\xi+1)C_s}\frac{a\omega_{ci}}{C_s}. \tag{10b}$$

Here we assume that the conducting end-plate allows a sufficient current to flow across the field lines to neutralize the ion space-charge as the ions move radially. Otherwise, the velocity of radial plasma flux would be limited by electrons [8] due to low electron conductivity across the field lines. This would also change estimate (5b) for the radial electric field.

The longitudinal ion flux ($\psi_\parallel$) and the longitudinal confinement time ($\tau_\parallel$) are readily

estimated from Eqs. (3), (5a), and (7):

$$\psi_{\parallel} \approx n v_{\parallel} a^2 \approx \frac{n a^2 C_s}{\xi(\xi+1)} \frac{C_s}{a\omega_{ci}}, \tag{11a}$$

$$\tau_{\parallel} \equiv \frac{L}{v_{\parallel}} \approx \xi(\xi+1) \frac{L}{C_s} \frac{a\omega_{ci}}{C_s}. \tag{11b}$$

It follows from Eqs. (10) and (11) that the ratio between the total longitudinal and radial ion fluxes is given by

$$\frac{\psi_{\perp}}{\psi_{\parallel}} = \frac{\tau_{\parallel}}{\tau_{\perp}} = \xi^2(\xi+1)^2. \tag{12}$$

We thus conclude that the longitudinal transport prevails when ξ is much smaller than unity, whereas the case $\xi \gg 1$ corresponds to predominantly radial transport.

III. ION DISTRIBUTION FUNCTION AND ION FLUXES

We start from the kinetic equation for the ion distribution function f, which reads:

$$\frac{\partial f}{\partial t} + \mathbf{v}\frac{\partial f}{\partial \mathbf{r}} + \frac{|e|}{m_i}\left(\mathbf{E} + \frac{1}{c}[\mathbf{v}\times\mathbf{B}_0]\right)\frac{\partial f}{\partial \mathbf{v}} = St(f), \tag{13}$$

where $\mathbf{E}$ is the ambipolar electric field and

$$St(f) \equiv n_0\sigma_{cx}\left(\delta(\mathbf{v})\int v' f d^3\mathbf{v}' - vf\right) + n_0\sigma_{el}\left(\frac{1}{\pi}\int \delta(v^2 - \mathbf{v}\cdot\mathbf{v}')f d^3\mathbf{v}' - vf\right) + \delta(\mathbf{v}) n n_0 \langle\sigma v\rangle_e . \tag{14}$$

The collision operator $St(f)$ describes the charge-exchange process, elastic scattering, and gas ionization by electron impact at the rate $\langle\sigma v\rangle_e$. The charge-exchange process "takes the ions away" at a rate $\sigma_{cx}v$ and returns them to the ion distribution at zero velocity. Elastic collisions "take the ions away" at a rate $\sigma_{el}v$ and return them isotropically distributed in the center of mass reference frame. As already pointed out in Sec. II, we can treat the cross-sections σ_{cx} and σ_{el} as constants since they are insensitive to the ion energy in the relevant energy range of up to few eV.

In order to solve Eq. (13), we will assume the following ordering

$$\omega_{ci} \gg n_0(\sigma_{cx} + \sigma_{el})v \gg n_0 \langle\sigma v\rangle_e \sim 1/\tau, \tag{15}$$

where τ is the characteristic discharge time. We also assume that

$$\rho_{Li} \ll a, \qquad \lambda \equiv \frac{1}{n_0(\sigma_{cx} + \sigma_{el})} \ll L. \tag{16}$$

These assumptions allow us to neglect, to lowest order, the spatial and time derivatives of f in Eq. (13) as well as the "ionization" term in the collision operator (14). As a result, Eq. (13) reduces to

$$\frac{|e|}{m_i}\left(\mathbf{E} + \frac{1}{c}[\mathbf{v} \times \mathbf{B}_0]\right)\frac{\partial f}{\partial \mathbf{v}} = n_0\sigma_{cx}\left(\delta(\mathbf{v})\int v' f d^3\mathbf{v}' - vf\right) + n_0\sigma_{el}\left(\frac{1}{\pi}\int \delta(v^2 - \mathbf{v}\cdot\mathbf{v}')f d^3\mathbf{v}' - vf\right). \tag{17}$$

It should be noted that this equation automatically conserves the number of particles since both its left-hand side and its right-hand side vanish after integration over the velocity space. The distribution function f is normalized by the relation:

$$\int f d^3\mathbf{v} = n, \tag{18}$$

where n is the plasma density. The particle balance condition, obtained by velocity integration of Eq. (13), gives a continuity equation for n:

$$\frac{\partial n}{\partial t} + \frac{1}{r}\frac{\partial}{\partial r}(r j_r) + \frac{\partial j_z}{\partial z} = n n_0 \langle \sigma v \rangle_e, \tag{19}$$

where

$$j_r = \int f v_r d^3\mathbf{v}, \tag{20a}$$

$$j_z = \int f v_z d^3\mathbf{v}, \tag{20b}$$

and (r, φ, z) are cylindrical coordinates with the z-axis pointing in the direction of the magnetic field $\mathbf{B}_0$.

It should be noted that the radial ion flux j_r is related to the ion-neutral friction force by the momentum balance condition. We will see that this relationship simplifies the calculation of j_r considerably. The momentum balance condition has the form

$$-\frac{|e|}{m_i}\left(n\mathbf{E} + \frac{1}{c}[\mathbf{j} \times \mathbf{B}_0]\right) = -n_0(\sigma_{cx} + \sigma_{el})\int \mathbf{v} v f(\mathbf{v}) d^3\mathbf{v} + \frac{n_0\sigma_{el}}{\pi}\int \mathbf{v} d^3\mathbf{v}\int \delta(v^2 - \mathbf{v}\cdot\mathbf{v}')f(\mathbf{v}')d^3\mathbf{v}', \tag{21}$$

that can be obtained by integrating both sides of Eq. (17) over the velocity space with a multiplier $\mathbf{v}$. The φ-component of Eq. (21) gives

$$j_r = -\frac{n_0(\sigma_{cx}+\sigma_{el})}{\omega_{ci}}\int v_\varphi v f(\mathbf{v})d^3\mathbf{v} + \frac{n_0\sigma_{el}}{\pi\omega_{ci}}\int K_\varphi(\mathbf{v}')f(\mathbf{v}')d^3\mathbf{v}', \tag{22}$$

where

$$\mathbf{K}(\mathbf{v}') \equiv \int \delta(v^2 - \mathbf{v}\cdot\mathbf{v}')\mathbf{v}d^3\mathbf{v}. \tag{23}$$

We note that the vector $\mathbf{K}$ is necessarily parallel to $\mathbf{v}'$, the only preferred direction in Eq. (23). We can therefore put

$$\mathbf{K} = \alpha\mathbf{v}', \tag{24}$$

with

$$\alpha = \frac{1}{v'^2}\int \delta(v^2 - \mathbf{v}\cdot\mathbf{v}')\mathbf{v}\cdot\mathbf{v}'d^3\mathbf{v}. \tag{25}$$

It is convenient to use spherical coordinates with the symmetry axis along $\mathbf{v}'$ to perform integration in Eq. (25):

$$\alpha = \frac{2\pi}{v'}\int_0^\infty v^3 dv \int_0^\pi \delta(v^2 - vv'\cos\theta)\cos\theta\sin\theta d\theta = \frac{2\pi}{v'^3}\int_0^{v'} v^3 dv = \frac{\pi v'}{2}. \tag{26}$$

Equations (22)-(25) combine into the following expression for j_r that we will later use instead of Eq. (20a):

$$j_r = -\frac{n_0(2\sigma_{cx}+\sigma_{el})}{2\omega_{ci}}\int v_\varphi v f d^3\mathbf{v}. \tag{27}$$

We now return to Eq. (17) and transform it to a reference frame that moves with the $\mathbf{E}\times\mathbf{B}$-drift velocity

$$\mathbf{u}_E \equiv \mathbf{e}_\varphi u_E = -\mathbf{e}_\varphi \frac{|e|E_r}{m_i\omega_{ci}}. \tag{28}$$

This transformation conveniently eliminates the term $E_r\partial f/\partial v_r$ from the left-hand side of Eq. (17). We normalize the velocity to $|u_E|$, so that

$$v_r = |u_E|V_\perp\cos\psi, \tag{29}$$

$$v_\varphi = |u_E|V_\perp\sin\psi + u_E, \tag{30}$$

$$v_z = \frac{E_\parallel}{|E_\parallel|}|u_E|V_z, \tag{31}$$

where $(V_\perp, \psi, V_z)$ are dimensionless cylindrical velocity-space variables. In these new variables, Eq. (17) takes the form

$$
\begin{aligned}
&-\frac{1}{\xi^2}\frac{\omega_{ci}}{|\omega_{ci}|}\frac{|E_r|}{|E_\parallel|}\frac{\partial f}{\partial \psi} = -\frac{1}{\xi^2}\frac{\partial f}{\partial V_z} - \left(1 + V^2 + 2\frac{u_E}{|u_E|}V_\perp \sin\psi\right)^{1/2} f \\
&+ \frac{\sigma_{cx}}{\sigma_{cx}+\sigma_{el}}\delta(V_\perp\cos\psi)\delta\left(V_\perp\sin\psi + \frac{u_E}{|u_E|}\right)\delta(V_z) \\
&\times \int \left(1 + V_\perp'^2 + V_z'^2 + 2\frac{u_E}{|u_E|}V_\perp'\sin\psi'\right)^{1/2} f(\mathbf{V}')V_\perp' dV_\perp' d\psi' dV_z' \\
&+ \frac{\sigma_{el}}{\pi(\sigma_{cx}+\sigma_{el})}\int V_\perp' dV_\perp' d\psi' dV_z' f(\mathbf{V}') \\
&\times \delta\left[V_\perp^2 + V_z^2 + \frac{u_E}{|u_E|}(V_\perp\sin\psi - V_\perp'\sin\psi') - V_z V_z' - V_\perp V_\perp'\cos(\psi-\psi')\right], \qquad (32)
\end{aligned}
$$

where

$$
\xi \equiv \left[n_0(\sigma_{cx}+\sigma_{el})\frac{m_i u_E^2}{|eE_\parallel|}\right]^{1/2}. \qquad (33)
$$

Note that this definition of ξ agrees with that of Eq. (8) if we use estimates for $E_\parallel$ and E_r given by Eq. (5).

In accordance with the ordering given by Eq. (15), we represent f as:

$$
f = f_0 + f_1, \qquad (34)
$$

where f_0 is the gyro-averaged distribution function and f_1 is a small ψ-dependent correction that is higher order in $1/\omega_{ci}$. We note that we would need f_1 to calculate j_r from Eq. (20a). However, f_0 is actually sufficient to calculate both j_z and j_r if we use Eq. (20b) for j_z and Eq. (27) instead of (20a) for j_r. We then obtain

$$
j_z = 2\pi u_E^4 \frac{E_\parallel}{|E_\parallel|}\int V_z f_0(V_\perp; V_z) V_\perp dV_\perp dV_z, \qquad (35)
$$

$$
\begin{aligned}
j_r &= u_E^4 \xi^2 \frac{|E_\parallel|}{E_r}\frac{2\sigma_{cx}+\sigma_{el}}{2(\sigma_{cx}+\sigma_{el})}\int f_0(V_\perp; V_z) V_\perp dV_\perp dV_z \\
&\quad\times \int_0^{2\pi}(1 + V_\perp\sin\psi)\left(1 + V_\perp^2 + V_z^2 + 2V_\perp\sin\psi\right)^{1/2} d\psi. \qquad (36)
\end{aligned}
$$

In order to find f_0, we average Eq. (32) over ψ, which eliminates the dominant term $\omega_{ci}\partial f/\partial\psi$. We then replace f by f_0 in the remaining terms to obtain an equation for f_0:

$$
\begin{aligned}
&-\frac{1}{\xi^2}\frac{\partial f_0}{\partial V_z} - W_1(V_\perp; V_z) f_0 + \frac{\sigma_{el}}{\pi(\sigma_{cx}+\sigma_{el})}\int W_2(V_\perp; V_z; V_\perp'; V_z') f_0(V_\perp'; V_z') V_\perp' dV_\perp' dV_z' \\
&+ \frac{\sigma_{cx}}{\sigma_{cx}+\sigma_{el}}\delta(V_\perp - 1)\delta(V_z)\int W_1(V_\perp'; V_z') f_0(V_\perp'; V_z') V_\perp' dV_\perp' dV_z' = 0, \qquad (37)
\end{aligned}
$$

where

$$W_1(V_\perp; V_z) \equiv \int_0^{2\pi} \left(1 + V_\perp^2 + V_z^2 + 2V_\perp \sin\psi\right)^{1/2} \frac{d\psi}{2\pi}, \tag{38}$$

$$W_2(V_\perp; V_z; V_\perp'; V_z') \equiv \int_0^{2\pi} \frac{d\psi}{2\pi}$$
$$\times \int_0^{2\pi} \delta\left[V_\perp^2 + V_z^2 + V_\perp \sin\psi - V_\perp' \sin\psi' - V_z V_z' - V_\perp V_\perp' \cos(\psi - \psi')\right] d\psi'. \tag{39}$$

This equation suggests that f_0 must have the following structure:

$$f_0 = \frac{n}{2\pi |u_E|^3} \left[\delta(V_\perp - 1) G(V_z) + H(V_\perp, V_z)\right], \tag{40}$$

where H is a smooth function of $V_\perp$. Indeed, we need a δ-function piece in f_0 to balance the corresponding term in Eq. (37). On the other hand, a smooth part of the distribution (H) is needed to balance the term with W_2 in Eq. (37). This term is a smooth function of $V_\perp$ even for a peaked f_0 since it involves integration of f_0 over the entire velocity space. In terms of G and H, the normalization condition (18) translates into

$$\int G dV_z + \int H V_\perp dV_\perp dV_z = 1. \tag{41}$$

The two independent balance conditions for the peaked and smooth terms in Eq. (37) give a set of two coupled equations for G and H:

$$\frac{1}{\xi^2}\frac{\partial G}{\partial V_z} + W_1(1; V_z) G - \frac{\sigma_{cx}}{\sigma_{cx} + \sigma_{el}} \delta(V_z) \int W_1(1; V_z') G(V_z') dV_z'$$
$$= \frac{\sigma_{cx}}{\sigma_{cx} + \sigma_{el}} \delta(V_z) \int W_1(V_\perp'; V_z') H(V_\perp'; V_z') V_\perp' dV_\perp' dV_z', \tag{42}$$

$$\frac{1}{\xi^2}\frac{\partial H}{\partial V_z} + W_1(V_\perp; V_z) H - \frac{\sigma_{el}}{\pi(\sigma_{cx} + \sigma_{el})} \int W_2(V_\perp; V_z; V_\perp'; V_z') H(V_\perp'; V_z') V_\perp' dV_\perp' dV_z'$$
$$= \frac{\sigma_{el}}{\pi(\sigma_{cx} + \sigma_{el})} \int W_2(V_\perp; V_z; 1; V_z') G(V_z') dV_z'. \tag{43}$$

Equation (42) together with the normalization condition (18) allows us to readily express G in terms of H:

$$G(V_z) = \exp\left[-\xi^2 \int_0^{V_z} W_1(1; V_z') dV_z'\right] \Theta(V_z) \left(1 - \int H(V_\perp, V_z) V_\perp dV_\perp dV_z\right)$$
$$\times \left(\int_0^\infty \exp\left[-\xi^2 \int_0^{V_z} W_1(1; V_z') dV_z'\right] dV_z\right)^{-1}, \tag{44}$$

where Θ is a step function. This expression allows us to reduce Eq. (43) to an equation for $H(V_\perp; V_z)$ alone. We note that, in the absence of elastic scattering ($\sigma_{el} = 0$), Eq. (43) has a simple solution $H = 0$. Then Eqs. (40) and (44) with $H = 0$ give an analytic expression for the ion distribution. In the presence of both, charge-exchange and elastic collisions, Eqs. (43) and (44) have to be solved numerically. We plan to perform these calculations and describe them elsewhere. However, the dependence of j_r and j_z on plasma parameters in the most representative limiting cases can be obtained even without solving these equations. The shape of the distribution function enters j_r and j_z only via form-factor multipliers [see coefficients α_z and α_r defined by Eqs.(50) and (54)].

Distribution function and ion flux for predominantly longitudinal transport ($\xi \ll 1$)

In order to treat this limiting case, we use the following rescaling transformation:

$$g \equiv G/\xi, \qquad h \equiv H/\xi^3, \tag{45}$$

$$s_z \equiv \xi V_z, \qquad s_\perp \equiv \xi V_\perp. \tag{46}$$

We then put $\xi = 0$ in the transformed Eqs. (43) and (44) to obtain:

$$g(s_z) = \exp\left[-\frac{s_z^2}{2}\right]\Theta\left(s_z\right)\sqrt{\frac{2}{\pi}}\left(1 - \int h(s'_\perp, s'_z)s'_\perp ds'_\perp ds'_z\right), \tag{47}$$

$$\frac{\partial h}{\partial s_z} + h\sqrt{s_\perp^2 + s_z^2} - \frac{2\sigma_{el}}{\pi(\sigma_{cx} + \sigma_{el})}\int \frac{h(s'_\perp; s'_z)s'_\perp ds'_\perp ds'_z}{\sqrt{s_\perp^2 s_\perp'^2 - \left[s_\perp^2 + s_z^2 - s_z s'_z\right]^2}}$$
$$= \frac{2\sigma_{el}}{(\sigma_{cx} + \sigma_{el})|s_z|}\exp\left[-\frac{(s_\perp^2 + s_z^2)^2}{2s_z^2}\right]\Theta\left(s_z\right)\sqrt{\frac{2}{\pi}}\left(1 - \int h(s_\perp, s_z)s_\perp ds_\perp ds_z\right). \tag{48}$$

It is important that the only parameter in these equations is σ_{el}/σ_{cx}, which makes both $g(s_z)$ and $h(s_\perp; s_z)$ universal functions for a given ratio σ_{el}/σ_{cx}. As σ_{el}/σ_{cx} is typically an order of unity quantity, the characteristic values for $s_\perp$, s_z, g, and h in Eqs. (47) and (48) are also order of unity.

The parallel ion flux defined by Eq. (35) can now be presented in the form:

$$j_z = \alpha_z \frac{n|u_E|}{\xi}\frac{E_\parallel}{|E_\parallel|} = \alpha_z n\left[\frac{|eE_\parallel|}{m_i n_0(\sigma_{cx} + \sigma_{el})}\right]^{1/2}\frac{E_\parallel}{|E_\parallel|}, \tag{49}$$

with

$$\alpha_z \equiv \sqrt{\frac{2}{\pi}}\left(1 - \int h s_\perp ds_\perp ds_z + \sqrt{\frac{\pi}{2}}\int h s_z s_\perp ds_\perp ds_z\right). \tag{50}$$

The radial ion flux is negligible at $\xi \ll 1$ since it is smaller than j_z by a factor ξ^2.

Distribution function and ion flux for predominantly radial transport ($\xi \gg 1$)

In this limiting case, the terms $\partial G/\partial V_z$ and $\partial H/\partial V_z$ are negligible in Eqs. (42) and (43). It then follows from Eqs. (42) and (41) that

$$G(V_z) = \delta(V_z)\left(1 - \int H(V'_\perp, V'_z) V'_\perp dV'_\perp dV'_z\right). \tag{51}$$

Substitution of this expression into Eq. (43) gives a universal equation for $H(V_\perp; V_z)$:

$$\begin{aligned} &W_1(V_\perp; V_z)H - \frac{\sigma_{el}}{\pi(\sigma_{cx}+\sigma_{el})}\int W_2(V_\perp; V_z; V'_\perp; V'_z) H(V'_\perp; V'_z) V'_\perp dV'_\perp dV'_z \\ &= \frac{\sigma_{el} W_2(V_\perp; V_z; 1; 0)}{\pi(\sigma_{cx}+\sigma_{el})}\left(1 - \int H(V'_\perp, V'_z) V'_\perp dV'_\perp dV'_z\right). \end{aligned} \tag{52}$$

The characteristic values of H, $V_\perp$, and V_z are all order of unity in this equation.

Taking into account (36) and (51), we find that the radial ion flux is given by

$$j_r = \alpha_r n |u_E| \xi^2 \frac{|E_\parallel|}{E_r} = \alpha_r n n_0 (\sigma_{cx}+\sigma_{el}) \frac{u_E^2}{|\omega_{ci}|}\frac{E_r}{|E_r|}, \tag{53}$$

with

$$\begin{aligned} \alpha_r \equiv \frac{8}{3\pi}\frac{2\sigma_{cx}+\sigma_{el}}{(\sigma_{cx}+\sigma_{el})}\Bigg[1 - \int H V_\perp dV_\perp dV_z \\ + \frac{3}{32}\int H V_\perp dV_\perp dV_z \int_0^{2\pi} (1 + V_\perp \sin\psi)\left(1 + V_\perp^2 + V_z^2 + 2V_\perp \sin\psi\right)^{1/2} d\psi\Bigg]. \end{aligned} \tag{54}$$

We note that $H = 0$ and $\alpha_r = 16/3\pi$ in the absence of elastic scattering ($\sigma_{el} = 0$). The longitudinal ion flux is formally zero for the distribution function (51). In reality, j_z is, of course, finite, but it is suppressed by a large factor ξ^4 compared to j_r.

IV. PLASMA DENSITY PROFILES IN STEADY-STATE FLOWS

In this section, we use the results of Sec. III to analyze plasma density profiles under the assumptions that the gas ionization rate $\langle \sigma v \rangle_e$ and the electron temperature T_e are constant throughout the discharge. We can relate the ambipolar electric field to the density gradient, so that

$$\mathbf{E} = -\frac{T_e}{|e|}\frac{1}{n}\frac{\partial n}{\partial \mathbf{r}}. \tag{55}$$

In order to find the plasma density profile, we need to solve the continuity equation (19) in which the fluxes are self-consistently expressed in terms of $n(\mathbf{r}, t)$ via Eqs. (35), (36), and (55). We will use the "absorbing" boundary conditions at the end-plate and at the side walls:

$$n(a, z) = 0, \tag{56}$$

$$n(r, 0) = 0. \tag{57}$$

In addition, we put

$$n(r, L) = 0 \tag{58}$$

since the plasma density in the outgoing collisionless flow is much smaller than the density inside the source where the flow is collisional.

It should be noted that Eq. (19) for $n(\mathbf{r}, t)$ is invariant with respect to a rescaling transformation $n \to \alpha n$, despite the fact that this equation is nonlinear. Therefore, Eq. (19) determines just a functional dependence of n on $\mathbf{r}$ and t, but not the absolute value of the plasma density. In order to find the absolute value of n, we must solve the particle and power balance equations together.

The rescaling symmetry of Eq. (19) allows us to seek $n(\mathbf{r}, t)$ in the form

$$n(\mathbf{r}, t) = n(\mathbf{r})\mathrm{e}^{\gamma t}, \tag{59}$$

where γ is a constant. This expression indicates that, depending on our input parameters T_e and $\langle \sigma v \rangle_e$, we may have not just a steady-state solution with $\gamma = 0$, but also growing ($\gamma > 0$)

or decaying ($\gamma < 0$) density profiles. Clearly, solutions with $\gamma > 0$ describe an avalanche-type ionization that occurs when the losses due to plasma transport are insignificant. In reality, the exponential growth of plasma density will eventually seize due to the input power limitations, which once again indicates the need for self-consistent particle and power balance treatment.

In order to capture the key features of the plasma density profile in a technically simple way, we will analyze Eq. (19) in the two complimentary limiting cases: $\xi \ll 1$ and $\xi \gg 1$. In these cases Eq. (19) becomes effectively one-dimensional. As indicated above, the case $\xi \ll 1$ corresponds to predominantly longitudinal transport and the case $\xi \gg 1$ corresponds to predominantly radial transport. Taken together, these two solutions give sufficient qualitative understanding of all possible flows including the intermediate regime $\xi \sim 1$.

A Longitudinal transport

It is allowable to neglect j_r in Eq. (19) in the limit $\xi \ll 1$, which simplifies Eq. (19) to:

$$\gamma n + \frac{\partial j_z}{\partial z} = n_0 n \left\langle \sigma v \right\rangle_e , \tag{60}$$

where we use the representation (59) for n. In this equation, the longitudinal flux j_z is related to the density profile $n(z)$ by Eqs. (49) and (55), which give:

$$j_z = -\alpha_z n C_s \left(n n_0 (\sigma_{cx} + \sigma_{el}) \left| \frac{\partial n}{\partial z} \right| \right)^{-1/2} \frac{\partial n}{\partial z}. \tag{61}$$

We first consider a steady-state profile for which $\gamma = 0$, so that Eq. (60) takes the form:

$$-\frac{\partial \eta / \partial \zeta}{|\partial \eta / \partial \zeta|} \frac{\partial}{\partial \zeta} \left(\sqrt{\eta \left| \frac{\partial \eta}{\partial \zeta} \right|} \right) = \eta, \tag{62}$$

where η and ζ are dimensionless variables defined by:

$$\eta \equiv \frac{n}{max(n)}, \tag{63a}$$

$$\zeta \equiv \left(\frac{\langle \sigma v \rangle_e^2}{\alpha_z^2 C_s^2} (\sigma_{cx} + \sigma_{el}) \right)^{1/3} \int_0^z n_0 dz. \tag{63b}$$

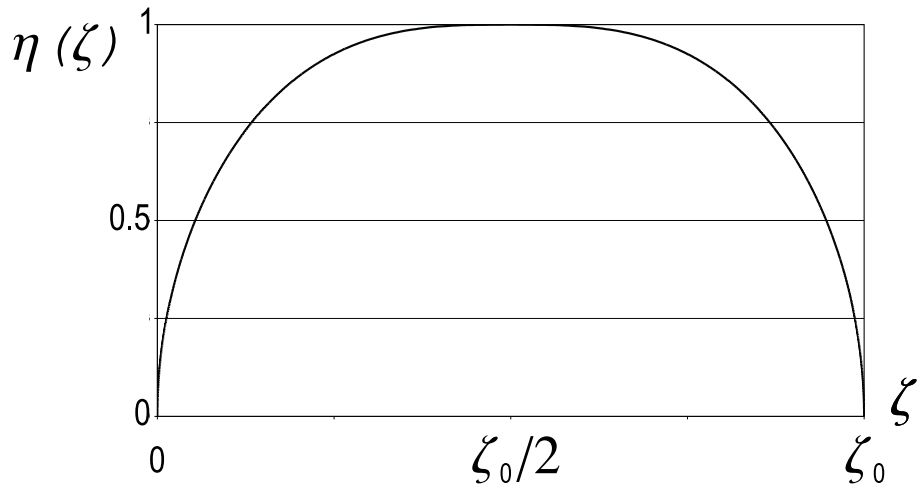

FIG. 3: Normalized longitudinal profile of the plasma density [plot of the solution given by Eqs. (67)].

We use a substitution

$$\frac{\partial \eta}{\partial z} = \Phi(\eta), \tag{64}$$

where $\Phi(\eta)$ is a new unknown function, to transform the second-order equation (62) to a first-order equation for Φ:

$$-|\Phi| \frac{\partial}{\partial \eta} \sqrt{\eta |\Phi|} = \eta. \tag{65}$$

A straightforward integration of this equation gives:

$$|\Phi(\eta)| = \frac{(1-\eta^3)^{2/3}}{\eta}, \tag{66}$$

where the integration constant has been determined from Eq. (63a), which requires that $\eta = 1$ at the point where $\Phi(\eta) = 0$.

Equations (64) and (66) allow us to construct a density profile that satisfies the boundary condition at the end-plate ($\eta(0) = 0$) and has $\eta = 0$ at some distance ζ_0 away from the end-plate. This solution is implicitly given by the following integrals:

$$\zeta(\eta) = \int_0^\eta \frac{x dx}{(1-x^3)^{2/3}} \qquad \text{for} \qquad 0 < \zeta < \zeta_0/2, \tag{67a}$$

$$\zeta(\eta) = \zeta_0/2 + \int_\eta^1 \frac{x dx}{(1-x^3)^{2/3}} \qquad \text{for} \qquad \zeta_0/2 < \zeta < \zeta_0, \tag{67b}$$

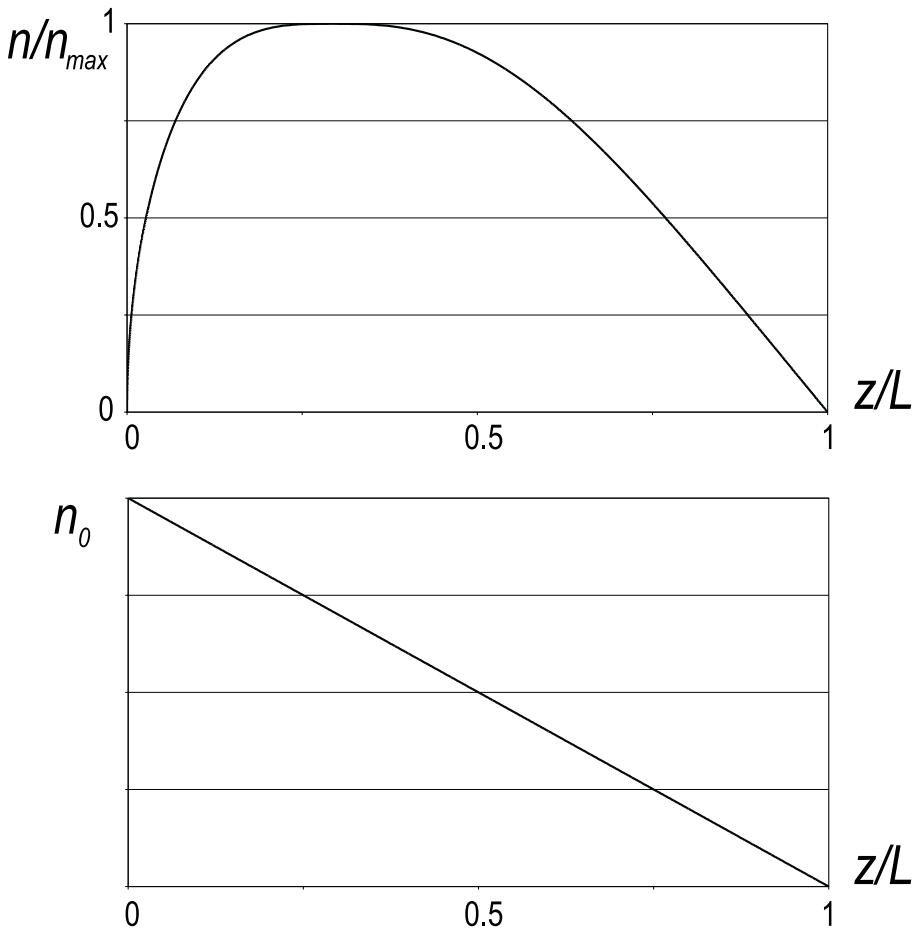

FIG. 4: Asymmetry in the longitudinal plasma density profile (upper plot) due to the gas density gradient in Knudsen flow (lower plot).

where

$$\zeta_0 \equiv 2\int_0^1 \frac{xdx}{(1-x^3)^{2/3}} = \frac{4\pi}{3\sqrt{3}}. \tag{68}$$

The plot of $\eta(\zeta)$ for this solution is shown in Fig. 3. Note that $\eta(\zeta)$ is a symmetric function. The corresponding density profile $n(z)$ is shown in Fig. 4. In contrast with $\eta(\zeta)$, the function $n(z)$ is not symmetric. The symmetry of the density profile breaks because of the gas density gradient along the tube.

It is important that ζ_0 is not a free parameter since it is fixed by Eq. (68). Equations (68) and (63b) show that the open-end boundary condition (58) requires a fixed amount of

gas to establish the steady-state regime. Namely,

$$\int_0^L n_0 dz = \frac{4\pi}{3\sqrt{3}} \left(\frac{\langle \sigma v \rangle_e^2}{\alpha_z^2 C_s^2} (\sigma_{cx} + \sigma_{el}) \right)^{-1/3} . \tag{69}$$

If the gas content is too high, so that

$$\int_0^L n_0 dz > \frac{4\pi}{3\sqrt{3}} \left(\frac{\langle \sigma v \rangle_e^2}{\alpha_z^2 C_s^2} (\sigma_{cx} + \sigma_{el}) \right)^{-1/3} , \tag{70}$$

then the ionization cannot be balanced by the ion transport, which formally means that a positive γ is required to satisfy the boundary conditions for Eq. (60). As a result, the plasma density grows in time under condition (70). Following the same logic, we conclude that the plasma density should decay if the gas content is too low to satisfy Eq. (69).

B Radial transport

In the case of predominantly radial transport ($\xi \gg 1$) the continuity equation reads

$$\gamma n + \frac{1}{r} \frac{\partial}{\partial r} (j_r r) = n_0 n \langle \sigma v \rangle_e , \tag{71}$$

where we again use representation (59). The relation between the radial flux and the density profile follows readily from Eqs. (53) and (55), which give:

$$j_r = -\alpha_r n C_s \frac{n_0 C_s^3 (\sigma_{cx} + \sigma_{el})}{n^2 |\omega_{ci}|^3} \frac{\partial n}{\partial r} \left| \frac{\partial n}{\partial r} \right| . \tag{72}$$

Similar to subsection IV A, we first construct a steady state solution of Eq. (71). We note that the density profile must be monotonic in steady-state regime, so that $\partial n/\partial r < 0$ and $j_r > 0$ in this solution. Indeed, any hollow profile would create an inward plasma flux towards the axis, which is not permissible in a steady-state.

Since the radial flux is a positive definite, we put $\partial n/\partial r = -|\partial n/\partial r|$ to transform Eq. (71) with $\gamma = 0$ to

$$\frac{1}{\rho} \frac{\partial}{\partial \rho} \left(\frac{\rho}{\eta} \left[\frac{\partial \eta}{\partial \rho} \right]^2 \right) = \eta. \tag{73}$$

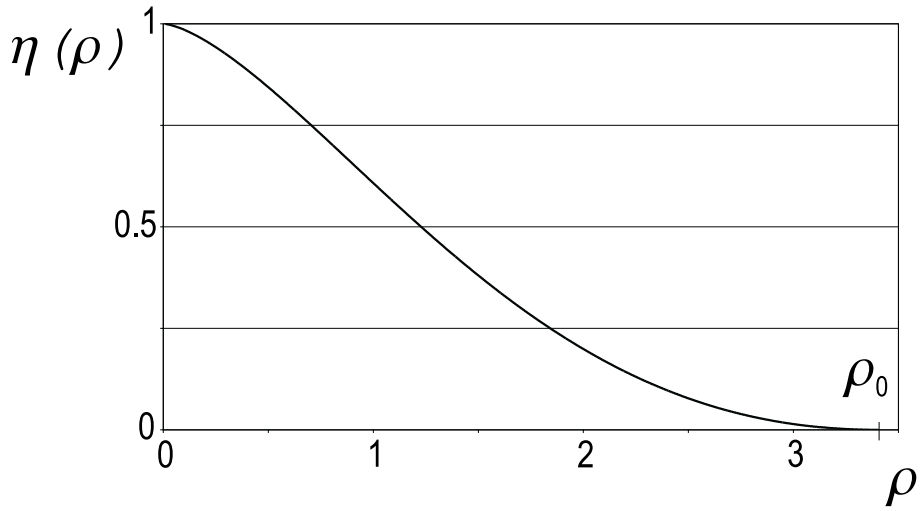

FIG. 5: Normalized radial profile of the plasma density [plot of the numerical solution of Eq. (73)].

Here, the dimensionless variables η and ρ are related to n and r by

$$\eta \equiv \frac{n}{n|_{r=0}} \tag{74a}$$

$$\rho \equiv \frac{|\omega_{ci}|}{C_s}\left(\frac{\langle\sigma v\rangle_e}{\alpha_r(\sigma_{cx}+\sigma_{el})C_s}\right)^{1/3} r. \tag{74b}$$

As the radial flux must vanish at $r \to 0$, we require

$$\frac{\partial\eta}{\partial\rho} = 0 \qquad \text{for} \qquad \rho = 0. \tag{75}$$

In addition to this, Eq. (74a) requires that

$$\eta = 1 \qquad \text{for} \qquad \rho = 0. \tag{76}$$

Equations (75) and (76) uniquely determine the solution of Eq. (73), which is presented in Fig. 5. The function $\eta(\rho)$ takes on zero value at $\rho = \rho_0 \approx 3.403$. In order to obtain a steady-state solution, condition $\eta(\rho_0) = 0$ must be compatible with the boundary condition (56), which determines the required ionization rate $\langle\sigma v\rangle_e$:

$$\langle\sigma v\rangle_e = \alpha_r C_s(\sigma_{cx}+\sigma_{el})\left(\frac{\rho_0}{a}\frac{C_s}{|\omega_{ci}|}\right)^3. \tag{77}$$

It is noteworthy, that in contrast with the case of longitudinal transport, Eq. (77) is independent of the gas density.

If the ionization rate differs from that given by Eq. (77), then a nonzero value of γ is needed to construct a solution. Note that $\langle \sigma v \rangle_e$ and γ enter Eq. (71) in a combination $\langle \sigma v \rangle_e - \gamma / n_0$. Therefore, we can readily satisfy the wall boundary condition (56) by putting

$$\gamma = n_0 \langle \sigma v \rangle_e - \alpha_r C_s n_0 (\sigma_{cx} + \sigma_{el}) \left(\frac{\rho_0}{a} \frac{C_s}{|\omega_{ci}|} \right)^3 . \tag{78}$$

It is interesting that the normalized density profile shown in Fig. 5 is independent of γ if we redefine ρ as

$$\rho \equiv \frac{|\omega_{ci}|}{C_s} \left(\frac{\langle \sigma v \rangle_e - \gamma / n_0}{\alpha_r (\sigma_{cx} + \sigma_{el}) C_s} \right)^{1/3} r. \tag{79}$$

In agreement with intuitive expectations, we find that the plasma density builds up exponentially ($\gamma > 0$) when the ionization rate exceeds the "steady-state" value (77) and decays ($\gamma < 0$) when the ionization is too slow to satisfy Eq. (77).

V. DISCUSSION

This section contains few remarks concerning limitations of our model and possible experimental implications of our results.

In this paper we have focused on the particle balance aspect of the magnetized plasma source operation. We have deliberately left out any discussion of the power balance, including the issue of rf-absorption and the problem of electron kinetics. It is clear that power balance analysis should ultimately be added to construct a fully consistent discharge model. In particular, such a model should allow us to analyze the discharge stability in the spirit of Ref. [10], where the stability problem was addressed at a phenomenological level. The remaining challenge is to combine the ideas of Ref. [10] with a first principle kinetic description of the plasma.

Our solution of the ion kinetic equation shows that the ion distribution function (40) is strongly peaked at $v_r^2 + v_\varphi^2 = u_E^2$ ($V_\perp = 1$) when charge-exchange collisions with cold neutral gas are the dominant ion collisions. It is noteworthy that the peak in the ion distribution function survives even in the regime when there are elastic ion-atom collisions in addition to charge-exchange collisions. We observe that elastic collisions do not broaden the peak, but

rather reduce its amplitude and add a "halo" component to the ion distribution. The reasons for peak broadening are the background gas temperature and ion-ion collisions. These factors become important only at a relatively high plasma density n. Otherwise, the background gas remains cold (although a population of energetic atoms may still arise [see below]). The role of ion-ion collisions should obviously increase with n since the corresponding collision frequency is proportional to n, whereas the ion-atom collision frequency is independent of n. At a sufficiently high plasma density, the ion-ion collisions will make the ion distribution Maxwellian with some temperature T_i and directed velocity $\mathbf{V}_i$. Despite the fact that this distribution differs form the one given by Eq. (40), the estimates for the ion fluxes presented in Sec. II will not change and the dependence of j_r and j_z on plasma parameters will remain the same in the limiting cases $\xi \ll 1$ and $\xi \gg 1$, except for the values of the form-factors α_r and α_z. It appears that the regime with relatively high plasma density is the one that is relevant to recent experiments [14–16]. The distribution function in Ref. [14–16] is reported to be of a Maxwellian-type suggesting that ion-ion collisions play an important role in its formation.

As we already mentioned in Sec. I, we neglected the plasma effect on the background gas profile in our analysis. This assumption again implies that the plasma density is not too high. We will now estimate the corresponding density limit for our model. In the absence of plasma, the Knudsen gas flux (q_0) through the system can be estimated as

$$q_0 \approx n_0 C_0 \frac{a}{L^2}, \tag{80}$$

where C_0 is the sound speed in the injected cold gas. The ion-atom collisions convert some of the cold atoms into fast atoms at the rate

$$q_{hot} \approx \nu n, \tag{81}$$

where ν is the ion-atom collision frequency. It is clear that the criterion for neglecting cold gas depletion is $q_{hot} \ll q_0$. Using the estimate for ν given by Eq. (7), we present this criterion in the form:

$$n \ll \frac{n_0 C_0}{\xi(\xi+1) L \omega_{ci}}. \tag{82}$$

We now note that, in a steady-state regime

$$q_{hot} \approx \frac{n_{hot}}{\tau_{hot}}, \tag{83}$$

where n_{hot} is the density of fast neutrals and τ_{hot} is their confinement-time. Similarly, the gas flux can be written as

$$q_0 \approx \frac{n_0}{\tau_0}, \tag{84}$$

where τ_0 is the confinement-time of a cold atom. It should also be noted that τ_{hot} is always smaller than τ_0 in the Knudsen flow. Therefore, the condition $q_{hot} \ll q_0$ guarantees that

$$n_{hot} \ll n_0. \tag{85}$$

However, despite their low density, the fast neutrals can still have larger pressure than the cold gas. The characteristic energy of a fast neutral is comparable to that of a plasma ion ($m_i v^2/2$). We can then estimate the fast neutral pressure as

$$P_{hot} \approx n_{hot}\frac{m_i v^2}{2} \approx n\nu\tau_{hot}\frac{m_i v^2}{2}. \tag{86}$$

If the atom collisions with the walls are elastic (with random scattering from the the wall), then the time atom stays in the quartz tube can be estimated as L^2/av. If the collisions lead to energy loss, then the corresponding energy life-time is roughly $a/\varepsilon v$, where ε is the energy loss fraction in a single collision. It is clear that τ_{hot} is the shortest of these two times, i.e. we can put

$$\tau_{hot} \approx \frac{a/v}{\varepsilon + a^2/L^2}. \tag{87}$$

We now combine Eqs. (86), (87), and (7) to obtain

$$P_{hot} \approx P_{pl}(\xi+1)^2\frac{a/L}{\varepsilon + a^2/L^2}, \tag{88}$$

where $P_{pl} = nT_e$ is the plasma pressure. This estimate can explain the observed gas pressure increase due to plasma production in helicon plasma sources. An example of the corresponding experimental data is presented in Fig. 6, which clearly shows a substantial

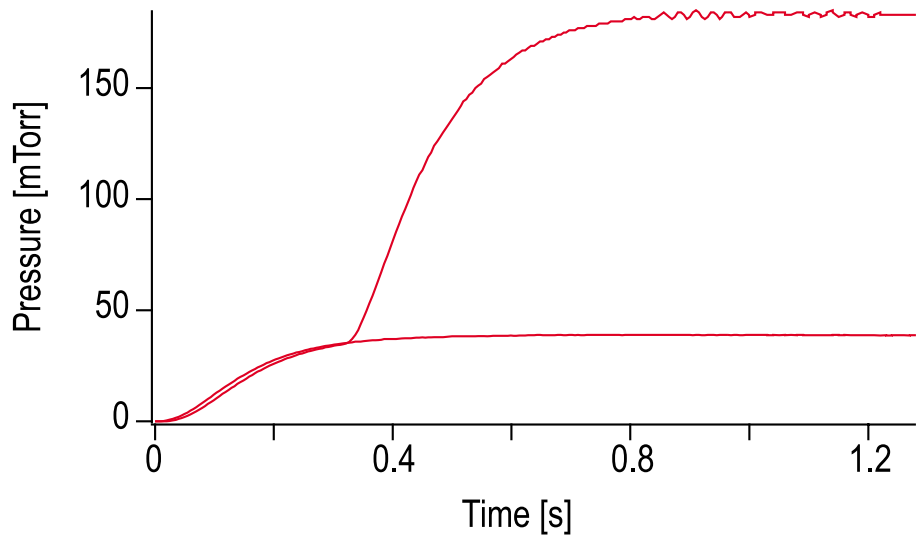

FIG. 6: Increase in the neutral gas (He) pressure near the end-plate due to plasma production. Lower curve: time evolution of gas pressure without plasma. Upper curve: time evolution of gas pressure with plasma. The discharge starts at $t = 300$ms. (courtesy of J.Squire and VASIMR team).

pressure increase that is much too big to be explained by the wall temperature increase. In this experiment, the background gas is He with a peak density $n_0 = 6 \cdot 10^{14}$ cm^{-3} and the plasma density measured in the outgoing flow is $n_{out} = 10^{12}$ cm^{-3}. The electron temperature is in the range of 5 eV. The characteristic value of plasma density inside the source is higher that n_{out} since the plasma density drops towards the open end (see Fig. 4). Taking $n \approx 10^{13}$ cm^{-3}, we find that the plasma pressure is roughly $P_{pl} \approx 60$ mTorr. In order to estimate parameter ξ [see Eq. (8)] we take $a \approx 5$ cm, $L \approx 100$ cm, $B_0 \approx 10^3$ G. The collision cross-sections in He are $\sigma_{el} \approx \sigma_{cx} \approx 2 \cdot 10^{-15}\ cm^{-2}$. The resulting value of ξ is 1.3. The fast neutral pressure observed in experiment is 150 mTorr (see Fig. 6). Equation (88) matches this value at $\varepsilon = 0.11$. Since the atom mass (m_i) in light gases is much smaller than the mass of the wall atoms (m_w), the energy transfer from the atoms to the wall is suppressed by roughly a factor of m_i/m_w, so that $\varepsilon \sim m_i/m_w$. For He atoms colliding with quartz tube walls this indicates that the fast neutral pressure is a good candidate to explain the substantial pressure increase. It is however difficult to be more conclusive at this point since Eq. (88) is a very rough estimate.

Another conceivable application of our results is a transition from peaked to hollow plasma density profiles observed in the helicon sources [17]. As discussed in Sec. IV B, the radial density profile is always peaked at the axis if the radial transport dominates. On the other hand, the radial density profile is that of the ionization source if the transport is predominantly longitudinal. Therefore, the profile should be hollow if the ionization rate is peaked off-axis and the transport is predominantly longitudinal. The choice between the two regimes depends on the value of the dimensionless parameter $\xi^2(\xi+1)^2$ [see Eq. (12)] that increases with the increase of n_0. Note that the transition reported in Ref. [17] was achieved primarily by reducing neutral gas pressure. This suggests that the observed effect may be partly associated with a transition from predominantly radial to predominantly longitudinal transport.

ACKNOWLEDGMENTS

This work was supported by the VASIMR Plasma Thruster project at NASA and by the U.S.Department of Energy Contract No. DE-FG03-96ER-54346. We thank Dr. Roger Bengtson, Dr. Franklin Chang-Diaz, and Mr. Jason Gibson for stimulating discussions. We also thank Dr. Jarred Squire for providing us with experimental data from VX-10 helicon plasma source. We appreciate the help of Mrs. Katharine Arefiev in editing the manuscript.

REFERENCES

[1] R.W.Boswell, Phys. Lett. **33A**, 457 (1970).

[2] R.W.Boswell, Plasma Phys. Control Fusion **26**, 1147 (1984).

[3] A.J.Perry, D.Vender, and R.W.Boswell, J. Vac. Sci. Technol. B **9**, 310 (1991).

[4] H.Kitagawa, A.Tsunoda, H.Shindo, and Y.Horiike, Plasma Sources Sci. Technol. **2**, 11 (1993).

[5] M.A.Liberman and A.J.Lichtenberg, "Principles of Plasma Discharges and Materials" (Wiley, New York, 1994).

[6] F.R.Chang Diaz, M.M.Hsu, T.F.Yang, "Rapid Mars Transit With Exhaust-Modulated Plasma Proplsion", *NASA Technical Paper* (National Aeronautics and Space Administration, Washington DC), 3539 (1995).

[7] F.R. Chang Diaz, J.P. Squire, A.V. Ilin, G.E. McCaskill, T.X. Nguyen, D.S. Winter, A.J. Petro, G.W. Goebel, L. Cassady, K.A. Stokke, C.E. Dexter, M.D. Carter, F.W. Baity, G.C. Barber, R.H. Goulding, D.O. Sparks, S.W. Schwenterly, R.D. Bengtson, B.N. Breizman, V.T. Jacobson, R.Z. Sagdeev, K. Karavasilis, S.V. Novakovski, A.A. Chan, T.W. Glover,"The Development of VASIMR Engine", in Proceedings of the International Conference on Electromagnetics in Advanced Applications (ICEAA'99, Torino, Italy, Sep. 13-17, 1999), IEEE, 99-102 (1999).

[8] F.F.Chen, J. Vac. Sci. Technol. A **10**, 1389 (1992).

[9] K.P.Shamrai, V.B.Taranov, Plasma Sources Sci. Technol. **5**, 474 (1996).

[10] K.P.Shamrai, Plasma Sources Sci. Technol. **7**, 499 (1998).

[11] D.Arnush, F.F.Chen, Phys. Plasmas **5**, 1239 (1998).

[12] B.N.Breizman and A.V.Arefiev, Phys. Rev. Lett. **84**, 3863 (2000).

[13] R.K.Janev, W.D.Langer, K.Evans, Jr. and D.E.Post, Jr., *Elementary Processes in Hydrogen-Helium Plasmas* (Springer-Verlag, Berlin, Heidelberg, 1987).

[14] E.E.Scime, P.A.Keiter, M.W.Zintl, M.M.Balkey, J.L.Kline, and M.E.Koepke, Plasma Sources Sci. Technol. **7**, 186 (1998).

[15] T.Nakano, K.P.Giapis, R.A.Gottscho, T.C.Lee, and N.Sadeghi, J. Vac. Sci. Technol. B **11**, 2046 (1993).

[16] N.Sadeghi, M.van de Grift, D.Vender, G.M.W.Kroesen, and F.J.de Hoog, Appl. Phys. Lett. **70**, 835 (1997).

[17] S.Yun, S.Cho, G.Tynan, and H.Chang, Phys. Plasmas **8**, 358 (2001).